








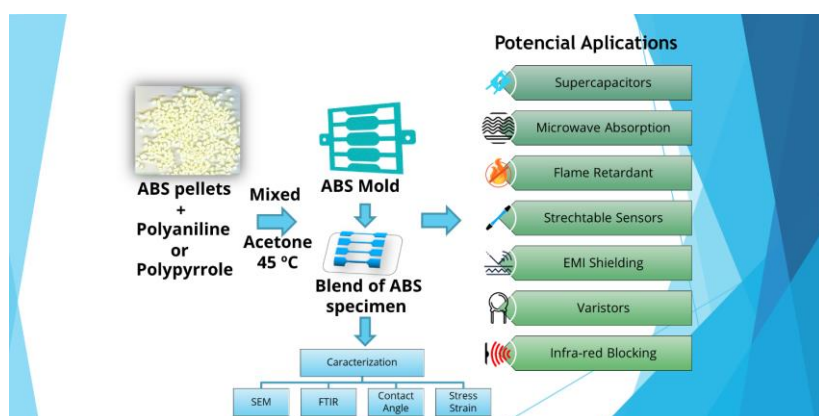
Full Paper | <http://dx.doi.org/10.17807/orbital.v16i3.19917>

# Preparation and Characterization of Blends with Small Amounts of Polyaniline and Polypyrrole Mixed with ABS Copolymer Matrix

Bianca Taína Ferreira <sup>c</sup>, Thamires Mariano <sup>a</sup>, Gabriel Badagnani de Carvalho\* <sup>a</sup>, Daniel Pasquini <sup>b</sup>, Rondinele Alberto dos Reis Ferreira <sup>b</sup>, Leila A. de Castro Motta <sup>b</sup>, and Luís Carlos de Moraes <sup>a</sup>

In this study, ABS copolymers were blended with doped polyaniline (PAni) and undoped polypyrrole (PPy) at concentrations of up to 2.5 % by weight. This allowed to understand how the mechanical and electrical resistivity properties of the ABS copolymer were affected by small quantities of these polymers. Scanning electron microscopy revealed that even with the smallest amounts of PAni or PPy added, significant morphological changes occur. The contact angle values revealed that there is a different limit in the addition of PAni or PPy to maximize the dispersive component effect. Mechanical analysis of the composites indicated that the addition of 0.625 % and 1.25 % PPy produced the highest values of Toughness, 3.87 MJ m<sup>-3</sup> and 3.89 MJ m<sup>-3</sup>, respectively. The stress at rupture varied from 57 to 61 MPa for ABS-PAni composites and from 25 to 61 MPa for ABS-PPy composites. In addition, the strain at break of ABS-PAni composites ranged from 4 to 7 %, while that of ABS-PPy composites varied from 5 to 12 %. Both ABS-PAni and ABS-PPy composites did not reveal significant changes by Thermogravimetric analysis (TGA). Finally, the electrical conductivity ( $\sigma$ ) of the composites increased six and eleven-fold, respectively, upon the addition of 2.5 % of doped PAni or undoped PPy, which were considered significant changes.

## Graphical abstract



## Keywords

ABS copolymer  
Composites  
Polyaniline  
Polypyrrole  
Electrical conductivity  
Mechanical properties

## Article history

Received 21 Dec 2023  
Revised 26 Jun 2024  
Accepted 08 Jul 2024  
Available online 26 Sep 2024

Handling Editor: Adilson Beatriz

## 1. Introduction

<sup>a</sup> Institute of Exact, Natural Sciences and Education (ICENE), Federal University of Triângulo Mineiro – UFTM, Uberaba, MG, Brazil. <sup>b</sup> Institute of Chemistry, Federal University of Uberlândia (UFU). Address: 2121 João Naves de Ávila Avenue, Santa Mônica, Uberlândia-MG, Brazil. <sup>c</sup> Department of Chemistry, Faculty of Philosophy, Sciences, and Letters of Ribeirão Preto, University of São Paulo (FFCLRP/USP), Ribeirão Preto-SP, Brazil. \*Corresponding author: +55 16 99228-7169. E-mail: [gabriel\\_badagnani@hotmail.com](mailto:gabriel_badagnani@hotmail.com)

Polymer composites and blends have been extensively studied to prepare various compounds for different applications. The method used to prepare them can significantly influence properties such as mechanical strength [1, 2] and electrical properties [3, 4]. As mentioned by Giaconi et al. [5], the synthesis methods and final morphology of the ABS polymer matrix can influence the mechanical properties. Therefore, it is important to make the right choice of polymers and methods of mixtures to achieve success in a specific application. If the desired property is mechanical and electrical resistance, can be mentioned that acrylonitrile-butadiene-styrene (ABS) is a good choice.

This class of copolymers contains three monomeric units: acrylonitrile, butadiene, and styrene. ABS is amorphous and therefore does not have crystallinity which implies that it does not have a true melting temperature. The final effect of the polymeric matrix is the result of the synergistic action between the types of meres present in the structure, as well as their relative proportions. For example, acrylonitrile directly influences hardness, chemical resistance, fatigue resistance, stiffness, and thermal deflection temperature. The styrene gives the plastic a shiny, waterproof surface, as well as hardness, rigidity, and greater ease of processing. Polybutadiene is a substance with elastomeric properties, providing toughness and ductility at low temperatures [6].

This polymer is heat-resistant and exhibits good toughness, which makes it widely applied in the automotive industry, pipes, appliance housings, 3-D printing systems, and other applications. ABS copolymer is a thermoplastic material that presents a glass transition temperature of around 105 °C and no melting temperature. It is generally mixed with other polymers to enhance some mechanical properties.

The other way, if the desired property to be reached is low electrical resistivity, the addition of carbon nanotubes [7, 8] and conductive polymers [9, 10] are viable options. Among the conductive polymers, polyaniline (PAni) and polypyrrole (PPy) are some of the most affordable options, making them suitable for large-scale applications.

Polyaniline is synthesized from aniline and its derivatives by using ammonium persulfate (APS) as the main oxidant. There are different oxidation states of polyaniline, with a specific name, such as i.e., leucoemeraldine (totally reduced form), pernigraniline (completely oxidized form), and emeraldine (around 50 % oxidized form). The salt-oxidized form of emeraldine is highly electrically conductive [11].

In polypyrrole synthesis, a wide variety of oxidative chemicals have been employed to initiate the polymerization process, including ferric compounds [12], ammonium persulfate [13], and others. Unlike the synthesis of PAni, the use of a dopant is not mandatory in the synthesis of PPy for electrical conductivity to occur.

For both, PAni and PPy, the presence of dopant and the type of dopant structure can increase or decrease the dispersion of these polymers in other polymer matrices. It is worth mentioning that doping with inorganic acids, such as hydrochloric acid, can make difficult the dispersions in more hydrophobic matrices. Some components, after doping, have structures that favor affinity with hydrophobic matrices and thus increase the dispersion of PAni and PPy. Furthermore, the dopant plays a fundamental role in reducing the electrical resistance of composites and blends produced from PAni or PPy [14]. The conductivity range of PAni is quite extensive and varies depending on certain factors, such as sample shape (film, powder, flakes, nanofibers, nanotubes, nanoflowers, etc). In addition, the type of dopant used is crucial. For

example, when hydrochloric acid is used as a dopant, the typical conductivity range is between 2.0 to 17 S/cm [15]. The same applies to PPy, which generally exhibits a conductivity range within the same range as observed for PAni [16].

From these observations, it is clear that a combination of variables is responsible for the electrical charge transference in a polymer matrix consisting of an insulation polymer and dispersed components (CNT, PAni, PPy, etc.) capable of conducting electrical charge over a difference in electrical potential ( $\Delta\phi$ ). Generally, when high molar mass polymers are dissolved in specific solvents, they produce a high viscosity medium that hinders the spreading of components to achieve a homogeneous bulk. This contributes to the enrichment of some regions that increase the electrical resistivity.

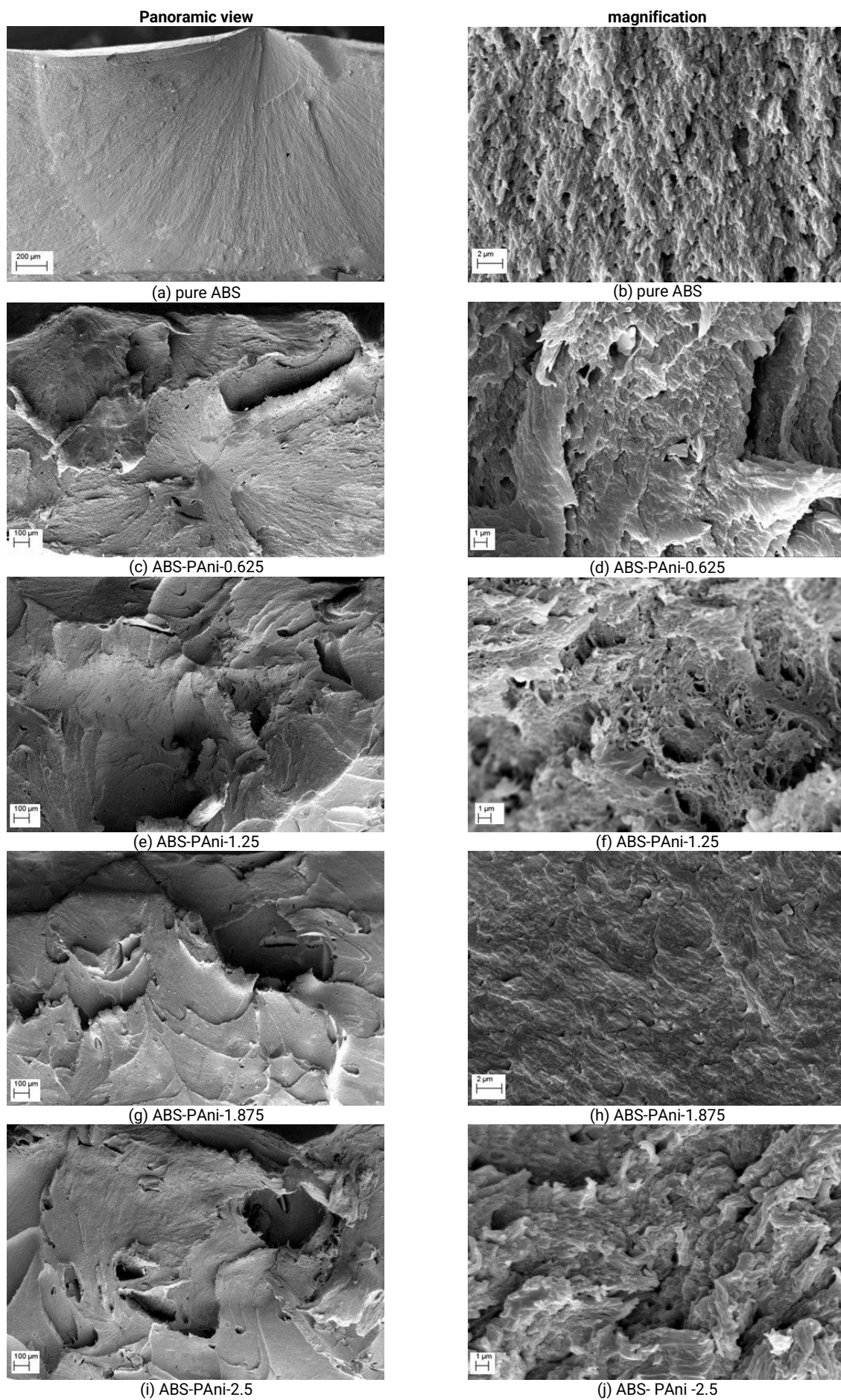
This opens up vast possibilities for applications, particularly in the formation of blends through the mixtures of copolymer ABS, PAni, and PPy with other conductive and thermoplastic polymers. Examples of different applications include ABS-PPy as flame retardant [17] microwave absorption and electrical properties of conducting ABS-polyaniline [18], supercapacitor based on nitrile butadiene rubber substrate and polypyrrole [19], stretchable strain sensors [20], Electromagnetic interference (EMI) shielding and infrared (IR) blocking by using polystyrene/polyaniline blend [21]. According to Foulger (1999), even though they have low electrical conductivity, some polymers can be applied as antistatic materials, low-temperature heaters, electromagnetic radiation shielding, and electric field grading [22].

In recent decades, conducting polymers (CPs) such as polyaniline and polypyrrole have garnered significant attention from scientists globally due to their exceptional properties, including tunable electrical, optical, and mechanical properties, along with ease of synthesis and high environmental stability compared to conventional inorganic materials. Despite the inherent limitations of CPs in their pristine form, their hybridization with other materials offers a promising solution to overcome these constraints. The synergistic effects of CP composites extend their applications across diverse fields such as electronics, medical, biomedical, and optoelectronics. This work aims to investigate how small amounts of PAni and PPy, below the percolation limit, can modulate the mechanical and electrical conductivity properties of an ABS copolymer matrix. As mentioned earlier, there is a wide variety of applications of interest using these polymers in electrically resistant polymer matrices. To achieve this goal, various characterization techniques were employed, including scanning electron microscopy (SEM), contact angle (CA), mechanical analysis (stress and strain at break), thermogravimetric analysis (TGA), and electrical measurements. These analyses provide a comprehensive understanding of the modifications induced by the addition of PAni and PPy in the ABS copolymer matrix, allowing for a precise assessment of how these changes may influence the performance and potential applications of these materials.

## 2. Results and Discussion

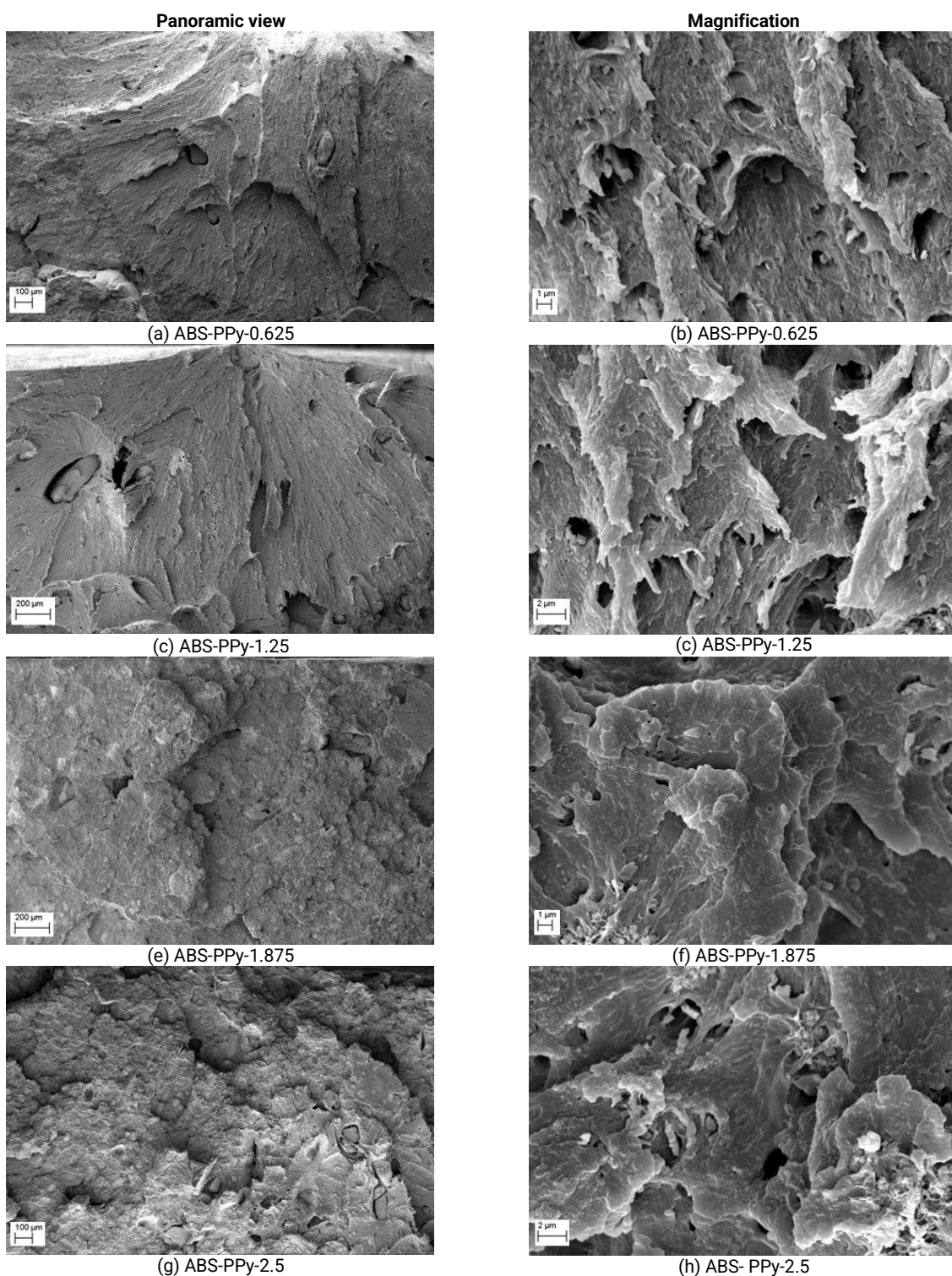
### 2.1 Scanning electron microscopy (SEM)

Figure 1 and Figure 2 display SEM images of the fractured surface of samples containing PAni and PPy, respectively. The PAni-composite micrographs presented in Figure 1 were performed with 120 times panoramic view and 10,000 times magnification.



(a) pure ABS (b) pure ABS (c) ABS-PAni-0.625 (d) ABS-PAni-0.625 (e) ABS-PAni-1.25 (f) ABS-PAni-1.25 (g) ABS-PAni-1.875 (h) ABS-PAni-1.875 (i) ABS-PAni-2.5 (j) ABS-PAni-2.5

**Fig.1.** SEM images of cold fractured regions for samples pure ABS and ABS-PANI.



**Fig. 2.** SEM images of cold fractured regions for sample ABS-PPy.

It is possible to observe from Figure 1-a that the fracture region appears smooth in the panoramic view. However, upon successive magnifications, in Figure 1-b, the surface shows a rough phase. After successive additions of PANi from 0.625 % up to 2.5 % (w/w) it is possible to observe significant variations in the shape of the fractured surface regions. These changes are related to the dispersion of PANi doped with HCl in the ABS matrix. In the doped state, PANi is brittle and fragments due to the shear imposed during mixing and this can contribute to forming porous holes.

Pores can be formed through various methods, depending on the methodology and process applied to induce their

formation. For instance, this can include the dispersion of polyaniline (PANi) doped with camphorsulfonic acid (CSA) in a polymer matrix, followed by the removal of the CSA [29]. Pores can also be created through solvent evaporation, where the solvent is eliminated by increasing the temperature, such as by placing samples in an oven, which creates void spaces within the sample. In this study, pore formation was observed in the fracture region, likely due to the detachment of undispersed PANi particles during the application of stress to break the material. This detachment left the observed void spaces, similar to pores.

According to Shackletfe and Han [28], PANi in the form of

an emeraldine base has solubility parameters ( $\delta$ ) that are  $\delta_d$  is 17.4 MPa<sup>1/2</sup>,  $\delta_p$  is 8.1 MPa<sup>1/2</sup>, and  $\delta_h$  is 10.7 MPa<sup>1/2</sup>, which allows calculating the total value of the Hildebrand's Parameter of  $\delta$  equal 22.2 MPa<sup>1/2</sup>. On the other hand, Peng et al. [30] showed that the Hildebrand's Parameter for ABS (1:2:4) has a total  $\delta$  equal to 23.7 MPa<sup>1/2</sup> while the partial contributions were  $\delta_d$  is 21.7 MPa<sup>1/2</sup>,  $\delta_p$  is 8.6 MPa<sup>1/2</sup>, and  $\delta_h$  is 3.9 MPa<sup>1/2</sup>. However, the dopant type of Pani affects these solubility parameters considerably, which is a sign that unfavorable miscibility happens when the total  $\delta$  of the polymer and the solvent are far. The solubility parameters of acetone are  $\delta$  equal 19.9 MPa<sup>1/2</sup>, with the partial contributions of  $\delta_d$  being 15.5 MPa<sup>1/2</sup>,  $\delta_p$  is 10.4 MPa<sup>1/2</sup> and  $\delta_h$  is 6.9 MPa<sup>1/2</sup> [31], which means acetone is not a suitable solvent for PANi, but a good solvent for ABS copolymer used here.

In this work, the other conducting polymer mixed with ABS was PPy in the undoped state. The micrographs are shown in Figure 2, with a panoramic view of 120 times and a magnification of 10,000 times.

Even in small amounts, PPy generated more aggregates than PANi as observed in the SEM images, and the fractured regions of ABS in the presence of PPy showed rougher surfaces than those observed with PANi. Similar to PANi, the use of acetone as a solvent for ABS may act as a non-solvent for PPy, which contributes to the formation of aggregates. The effect of solvent was observed by Merlini et al. [32], who mixed PPy with PVDF, and a smooth surface was observed when small amounts of PPy were added. However, with larger

amounts rougher surfaces were formed.

Solubilization of polymers in a suitable solvent can lead to an increase in viscosity. Typically, solubility parameters that are close in value are preferred. Several solvents were tested to dissolve PPy doped with DBSA. This acid has a long hydrophobic tail, which contributes to the dispersion of the doped polymer. However, hexafluoroisopropanol (HFIP) was considered the best solvent due to its highest viscosity [33].

In the literature, the solubility parameter of HFIP is found as  $\delta = 19.99$  MPa<sup>1/2</sup> with its partial contributions  $\delta_d$  is 14.17 MPa<sup>1/2</sup>,  $\delta_p$  is 2.41 MPa<sup>1/2</sup>, and  $\delta_h$  is 13.89 MPa<sup>1/2</sup> [34], which is very similar to PPy doped with DBSA. The HFIP solubility parameter is very similar to acetone, which means more affinity between ABS and PPy-DBSA with acetone. However, in this work, PPy is undoped. The solubility parameter presents its exception to the solubility criteria, as discussed as follows. As discussed by Mori and Barth [35], Poly (ethylene terephthalate) ( $\delta = 20.5$  MPa<sup>1/2</sup>) is not soluble in dioxane ( $\delta = 20.5$  MPa<sup>1/2</sup>) although it is soluble in HFIP. Although the solubility parameter is a highly valuable and potent tool for elucidating polymer properties in numerous solvents, its application is limited.

## 2.2 Mechanical Analysis

The mechanical properties of ABS polymer matrix before and after mixing with PANi and PPy were measured and the results are shown in Figure 3.

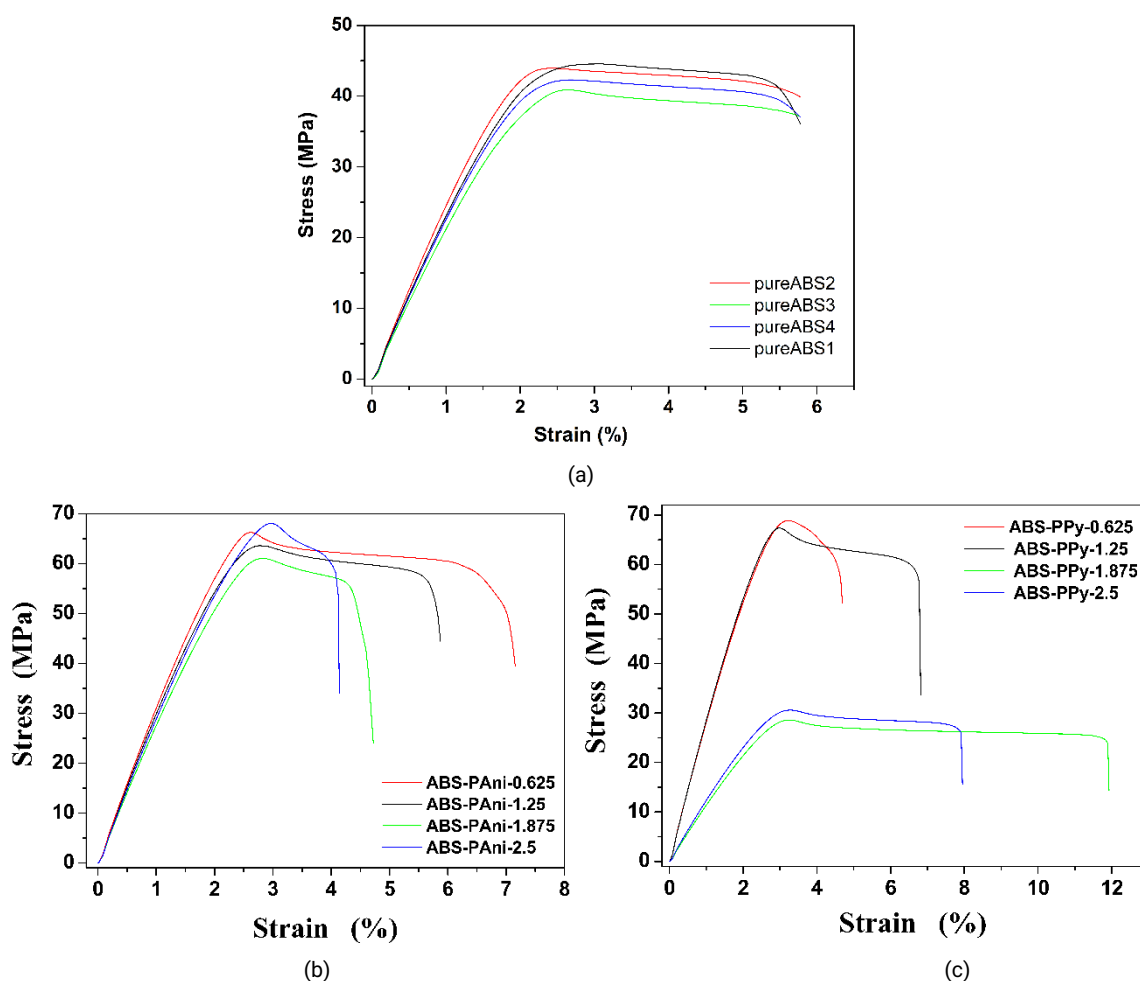


Fig. 3. Stress-Strain assays. (a) pure ABS, (b) ABS-PANi blend, (c) ABS-PPy blend.

Figure 3-a shows that Young's modulus, stress, and strain values are very close due to phase homogeneity and minimization of morphological changes that could influence the measurements, such as differences in microstructural features, cracks, bubbles, etc.

Figures 3-b and 3-c confirm that the addition of PANi to the polymer matrix results in less variability in mechanical behavior compared to samples containing PPy. However, in PPy samples, the maximum tensile strength is significantly reduced for concentrations greater than 1.25 %. In contrast,

for PANi blends, the maximum tensile strengths have similar values, unlike PPy blends. The strain at break for ABS-PANi showed a tendency to decrease with an increase in the amount of PANi in the ABS matrix, but this tendency was not observed for ABS-PPy strain at break. The stress and strain at fracture values obtained were similar to those reported by Greco and Dong [36], who did not use the solvent, but fused ABS in a Brabender machine.

The results that were obtained from the curves in Figures 3-a, 3-b, and 3-c are shown in Table 1.

**Table 1.** Young's modulus (YM), Maximum Tensile strength (MTS), Strain at fracture (%EL), and Toughness (T) of pure ABS, ABS-PANi and ABS-PPy. All results are with their respective standard deviation.

Samples	tensile strength (MPa)	strain at fracture (%EL)	Young's modulus (MPa)	Toughness (J m <sup>-3</sup> )x10 <sup>6</sup>
Pure ABS	42±2.84	6±0.45	2.596±239	2.12±0.12
ABS-PANi-0.625%	67±0.75	7±0.46	3.331±140	3.87±0.16
ABS-PANi-1.25%	60±3.23	5±0.67	3.197±79	2.34±0.05
ABS-PANi-1.875%	64±2.28	4±0.87	3.264±120	2.15±0.53
ABS-PANi-2.5%	66±1.76	5±0.61	3.184±53	2.35±0.38
ABS-PPy-0.625%	64±4.36	5±0.38	2.785±265	2.22±0.08
ABS-PPy-1.25%	70±1.04	7±0.61	3.240±88	3.89±0.39
ABS-PPy-1.875%	26±0.05	13±1.55	1.271±33	3.18±0.52
ABS-PPy-2.5%	30±0.90	8±0.20	1.321±44	1.81±0.10

The results in Table 1 allow us to see that the composite ABS-PANi-0.625 % showed the highest MTS, %EL, YM, and T within the PANi sample group. However, it is not the same for the PPy sample group. The highest TS, YM, and T belong to the ABS-PPy-1.25 %. The highest %EL occurred after the addition of 2.5 % of PPy. The values reported in Table 1 were similar to those obtained by Giaconi et al. [5], who demonstrated the energy dissipation behavior of various ABS samples depending on the plastic deformation mechanism. These results demonstrate the significant impact of even small amounts of PANi or PPy on the mechanical and electrical properties of the ABS copolymer, which will be discussed later.

The addition of PANi and PPy provided a significant increase in MTS compared with pure ABS matrix, the exceptions were to the samples ABS-PPy-1.875 and ABS-PPy-2.5. After the PPy addition of 1.25 % and 1.875 %, the T was increased by 83 % and 50 % in comparison to pure ABS. Debnath et al. [37] studied the effect of carbon black (CB) and nano clay (NC) aiming to increase the tensile strength (TS) and elongation of the blends produced by mixtures of ABS until 3 % of PANi and PPy. It was observed for ABS-PANi blends without CB and NC, the TS suffered a decrease of 42 % and 57 %, to TS and %EL, respectively. Considering ABS-PPy, an increase of 12 % for TS was observed, and a decrease of 63 % in %EL. These values are calculated considering that pure ABS had a TS of 19.7 MPa with 3% of CB. However, in this work, the pure ABS matrix showed a TS of 42 MPa, which represents two times greater than that obtained by Debnath et al. It was possible to verify that an increase in MTS and %EL were around 59 % and 17 % for ABS-PANi and 66 % and 50 % for ABS-PPy, respectively, higher than those reported by the authors. This demonstrates how important is the method of

mixture to form the blends.

### 2.3 Thermogravimetric analysis

The thermal stabilities were evaluated by thermogravimetric analysis (TGA) and the results are shown in Figure 4.

No significant changes were observed in Figures 4-a to 4-c, which represent the pure ABS sample as a reference. The degradation of ABS and ABS blends occurred in a single step and began at approximately 290 °C as demonstrated by DTG, according to observed by Attia (2016) [17]. As mentioned in the literature the PANi degradation initiates around 300 °C [38] and PPy starts near 227 °C [39] This temperature range is crucial as it determines the thermal stability of the sample. However, information regarding the degradation process beyond this range is outside the scope of this study.

These values of thermal stability indicate that PANi and PPy can be mixed with several thermoplastic resins without undergoing degradation and with good processability. Between 225 °C and 300 °C, the extent of mass variation is very small, indicating that it is unlikely to impair mechanical resistance.

PANi/PVDF blends were studied with an amount of PANi up to 30 % in weight by TGA. It was observed that for doped and redoped PANi; when the amount of PANi decreased to 12 % (w/w), the TG curves of PANi tended to approximate the TG curve of PVDF that depends on the concentration of the dopant [2]. These factors, including the concentration of PANi in the blend and the doping process, provide insight into the behavior of the TG curves observed in this work, up to the maximum concentration of 2.5 % of PANi and PPy added to ABS.

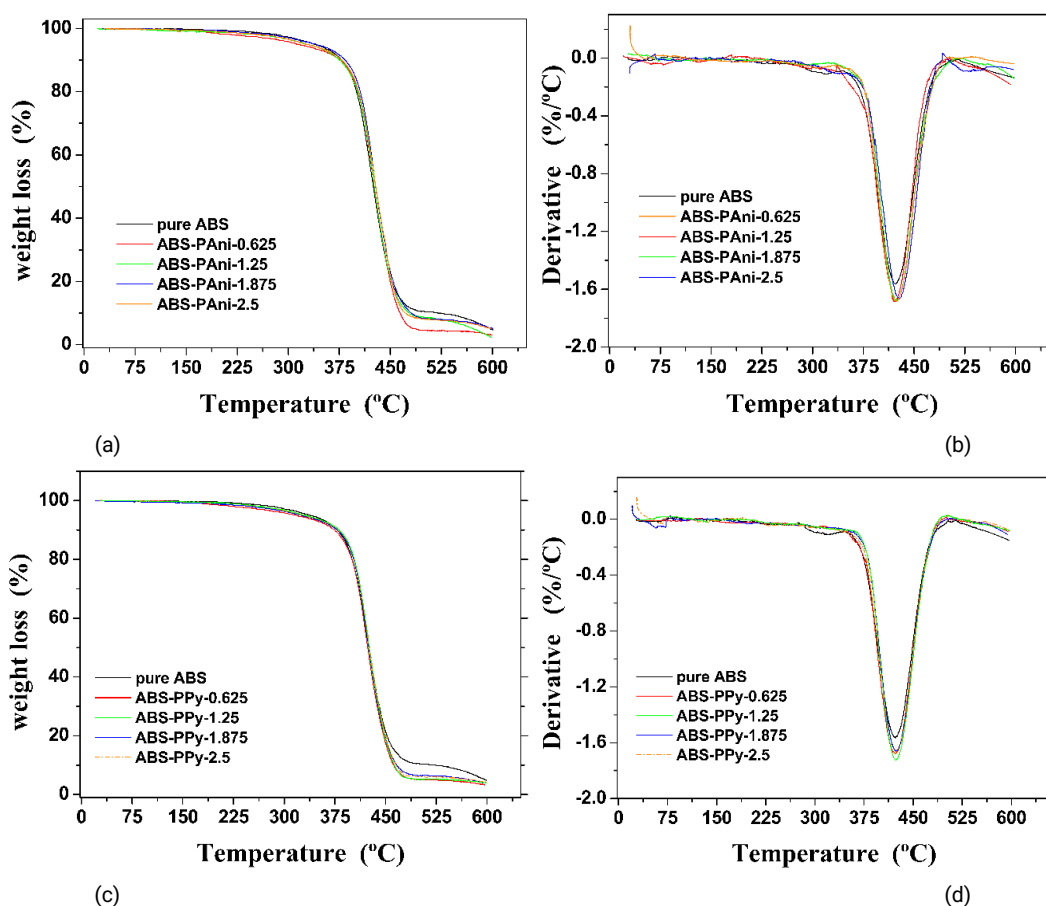


Fig. 4. Thermogravimetric analysis of the samples (a) pure ABS and ABS-PAni mixtures and (b) Derivative curves of samples. (c) pure ABS and ABS-PPy mixtures and (d) Derivative curves (DTG) of samples.

## 2.4 Contact angle

Understanding how these small amounts of PAni and PPy affected the surface of the ABS polymer matrix, the contact angle was carried out and the results are shown in Figure 5 and Table 2.

In Figure 5, only one image for each drop of solvent is shown. However, for calculation purposes, at least three

images were obtained. Generally, a contact angle near  $90^\circ$  or higher is indicative of a hydrophobic surface, and less than  $90^\circ$  is to hydrophilic surface.

In Table 2, the mean values with their respective standard deviations are shown. It is possible to see that the more hydrophilic the solvent the smaller the droplet angle.

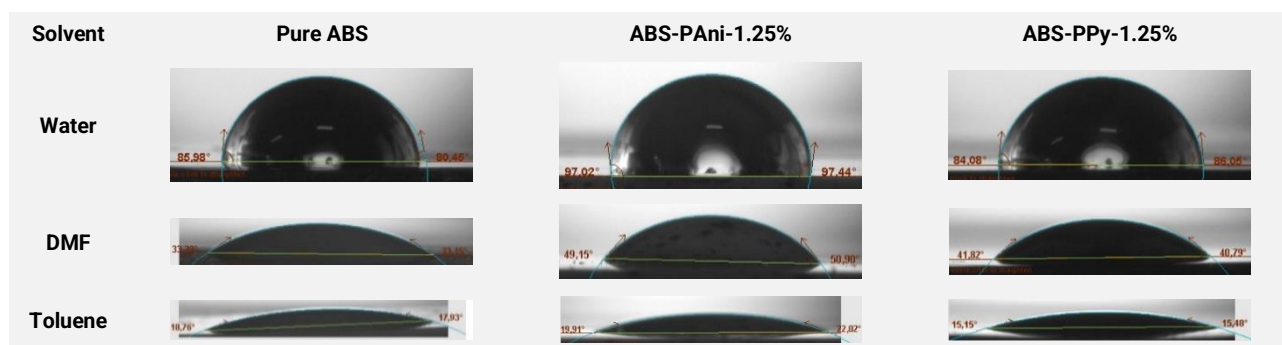


Fig. 5. Average contact angle (CA) over the composite surfaces with drops of water, DMF, and Toluene.

Solid surfaces are prone to contamination, which can lead to variations in contact angles. Belgacem et al. (2005) analyzed the surface energies of cellulosic fibers before and after cleaning, as results obtained using inverse gas chromatography (IGC) they observed an increase of up to 50 % in surface energy values [40]. This demonstrates the sensitivity of the highlights the importance of proper sample preparation before analysis.

In Table 2, the contact angles (CA) do not follow a specific sequence according to the concentrations of dispersed PAni or PPy in the ABS matrices. The results also indicate that the presence of PAni in the ABS blends should decrease the contact angle due to the doping process with HCl. However, several factors may to the variation observed, such as possible surface contamination or other factors contribute to this, possible surface contamination or other factors.

A study conducted by Blinova et al. (2008) demonstrated that the contact angles of water droplets on PANi surfaces vary depending on the pH. Angles near 44 ° are expected in a doped state, while angles of up to 78 ° can

be achieved in a partially doped state [15]. The presence of the chemical groups such as acrylonitrile (-C-N) and butadiene (-C-C=C-C-), may interfere with the protonation of PANi, resulting in partial doping.

**Table 2.** Contact angle, Surface tension (mN/m), and correlation coefficient ( $R^2$ ) for pure ABS, ABS-PAni, and ABS-PPy.

samples	Contact angle (degree)			Surface Tension (mN/m)			Correlation coefficient ( $R^2$ )
	Water	DMF	Toluene	$\gamma_s^p$	$\gamma_s^d$	$\gamma_s$	
Pure ABS	87.12 ± 2.25	33.68±1.13	17.97±0.45	7.5	21.3	28.8	0.9999
ABS-PAni-0.625%	86.69 ± 2.09	36.05±2.05	9.36±1.22	1.3	26.9	28.2	0.9762
ABS-PAni-1.25%	97.19 ± 2.00	50.45±1.02	22.26±0.42	3.1	22.4	25.5	0.9726
ABS-PAni-1.875%	101.89 ± 1.12	53.05±0.60	17.88±0.37	3.7	22.6	26.3	0.9978
ABS-PAni-2.5%	90.49 ± 2.02	40.19±0.87	16.63±0.68	5.1	22.0	27.1	0.9998
ABS-PPy-0.625%	101.60 ± 1.36	54.38±1.02	20.96±0.74	0.8	27.3	28.1	0.9615
ABS-PPy-1.25%	97.19 ± 2.05	50.45±2.45	22.26±0.31	2.8	24.4	27.2	0.9907
ABS-PPy-1.875%	87.45 ± 1.41	41.79±1.92	17.28±0.11	4.9	21.4	26.3	0.9983
ABS-PPy-2.5%	97.75 ± 2.15	50.24±0.82	19.07±1.34	9.6	17.5	27.1	0.9924

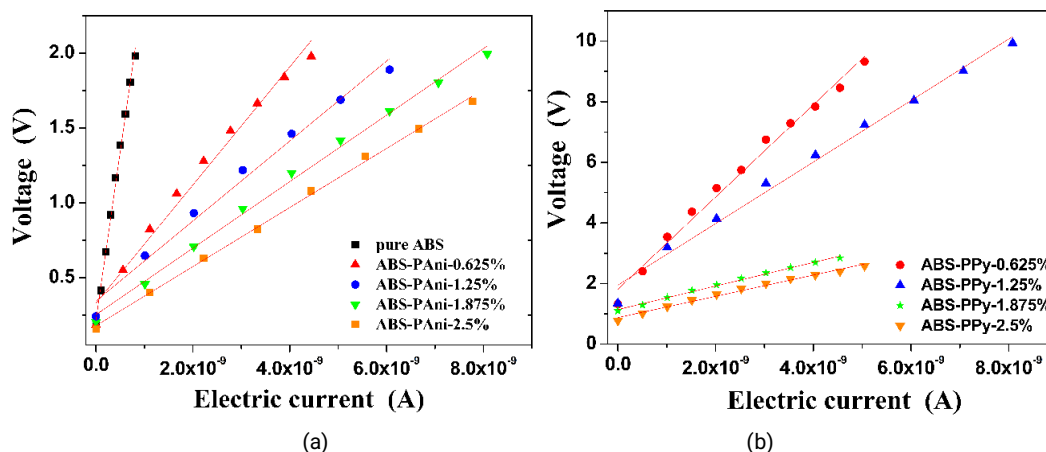
For pure ABS contact angles close to 78 ° (Cacho, 2014) and 81 ° (Olivera, 2016) have been found using water [41, 42]. These values are close to those found for PANi, which facilitates the mixture of phases to some extent. The CA results demonstrated that the hydrophobicity of the ABS polymer matrix increases with the addition of PANi above 0.625 %, while PPy makes the composites more hydrophobic at all concentrations. The increase of PPy by only 1.875 % in CA showed a significant difference, as in all other proportions a difference of 4 ° was observed regardless of the amount of PPy.

As can be observed, both conductive polymers showed higher contributions in dispersive surface tension ( $\gamma_s^d$ ) than their respective polar surface tensions ( $\gamma_s^p$ ). Successive additions of PANi caused an increase in the  $\gamma_s^p$ , although the

highest value (5.1 mN/m) was lower than that observed in the pure ABS polymer matrix (7.5 mN/m). For PPy, similar to those observed for PANi, successive additions caused an increase in  $\gamma_s^p$ . The highest amount added provided an increase of 28 % in  $\gamma_s^p$  when it is compared to that of pure ABS composite. As expected, the  $\gamma_s$  was very close to all samples when compared to pure ABS surface, due to the small amount of conductive polymers spread in the bulk blends.

## 2.5 Electrical resistance measurements

Electrical conductivity was also characterized to provide further information, aiding in the understanding of how even small quantities of PANi (or PPy) enhance this process. The results are presented in Figure 6.



**Fig. 6.** Electrical measurements. (a) pure ABS and ABS-PAni mixture and (b) pure ABS and ABS-PPy mixture.

From Figures 6-a (PANi) and 6-b (PPy), in both cases, an increase in conducting polymers contributed to a decrease in the electrical resistance. This can be better understood by analyzing the slope of each curve obtained by applying Ohm's first law.

According to Girotto and Santos [25], for circular samples that have dimensions as  $w < 4/10 * s$ , where "w" is the thickness and "s" is the spacing between probe tips (mm), the resistivity is calculated by equation (1), as follows:

$$\rho = R * w * 4.5324 \quad (1)$$

where  $\rho$  = electrical resistivity ( $\Omega \text{ m}$ ),  $R$  = electric resistance ( $\Omega$ ), and  $w$  = thickness of the sample in millimeters.

The electrical conductivity ( $\sigma$ ) was calculated as the reciprocal of the resistivity, as shown in equation (2):

$$\sigma = 1/\rho \quad (2)$$

where the unit of  $\sigma$  is  $\text{S m}^{-1}$ . After this, the results are shown in Table 3.

The electrical conductivity values corresponded to those within the semiconductor range ( $10^{-9}$  to  $10^{-2} \text{ S cm}^{-1}$ ) [43]. The ratio of electrical conductivities indicated that adding 2.5 % PANi to the ABS matrix resulted in an eleven-fold increase in electrical conductivity ( $\sigma$ ), which was the most significant improvement observed. Similarly, the best result with PPy was also achieved with a 2.5 % concentration, resulting in a six-fold



increase in  $\sigma$ , which is also a significant improvement. The type of solvents or their combination used in the preparation of composites or blends with conducting polymers has a significant impact on the electrical conductivity. The best result was obtained with blends containing ABS copolymer and PANi doped with dodecyl sulfonic acid (DBSA) prepared by the casting method using a mixture of solvents (m-cresol and chloroform), which showed a  $\sigma$  of  $9.35 \text{ S cm}^{-1}$  and still formed a flexible film [3]. Another work that only employed m-cresol reached a percolation threshold with only 2.66 % by

weight of CSA-doped poly(o-toluidine) and obtained an electrical conductivity of  $0.12 \text{ S cm}^{-1}$  [10]. Chen et al. [9] used only chloroform to solubilize the ABS copolymer and mixed it with PANi doped with DBSA. As a result, the electrical conductivity obtained at the percolation threshold, which was around 25 % by weight of PANi-DBSA, was around  $10^{-8} \text{ S cm}^{-1}$ . In this work, only acetone was used as a solvent and the highest value of electrical conductivity was  $5.52 \cdot 10^{-6} \text{ S m}^{-1}$ , which is equivalent to  $5.52 \cdot 10^{-8} \text{ S cm}^{-1}$ .

**Table 3.** Electrical measurements of pure ABS, ABS-PANi, and ABS-PPy mixtures.

samples	Electrical resistance (G $\Omega$ )	Coefficient correlation (R <sup>2</sup> )	Resistivity ( $\Omega \text{ m}$ )	Electrical conductivity $\sigma$ (S m <sup>-1</sup> )	Ratio $\sigma_{(\text{composites})}/\sigma_{(\text{pure ABS})}$
ABS puro	2.24	0.9974	2.03E+06	4.9249E-07	-----
ABS-PANi-0.625%	0.39	0.9806	3.54E+05	2.8286E-06	6
ABS-PANi-1.25%	0.26	0.9855	2.36E+05	4.2430E-06	9
ABS-PANi-1.875%	0.22	0.9956	1.99E+05	5.0144E-06	10
ABS-PANi-2.5%	0.20	0.9976	1.81E+05	5.5158E-06	11
ABS-PPy-0.625%	1.52	0.9884	1.38E+06	7.2577E-07	1
ABS-PPy-1.25%	1.01	0.9887	9.16E+05	1.0922E-06	2
ABS-PPy-1.875%	0.39	0.9949	3.54E+05	2.8286E-06	6
ABS-PPy-2.5%	0.35	0.9881	3.17E+05	3.1519E-06	6

Several studies have demonstrated the significance of the percolation threshold in explaining electrical conductivity [8, 44, 45]. The doping agents employed in these studies have an impact on the dispersion of PANi and PPy within the ABS matrix. Ahmed [44] investigated polyaniline doped with picric acid mixed with ABS copolymer and discovered that around 6 % by mass of PANi was necessary to achieve the percolation effect. It was observed that in the range of 0 % to 6 % of PANi, the electrical conductivity ranged from  $10^{-4} \text{ S cm}^{-1}$  to  $10^2 \text{ S cm}^{-1}$ .

The relationship between roughness and electrical resistance in ABS composite materials with conductive polymers such as PANi and PPy exhibits a complex interaction. The addition of PANi or PPy to ABS resulted in a significant increase in electrical conductivity, with the greatest improvements observed at concentrations of 2.5%. However, even in small amounts, PPy generated more aggregates than PANi, resulting in rougher surfaces in ABS-PPy composites. This surface roughness can impact the electrical resistance of the materials, especially on conducting surfaces, where increased roughness can elevate electrical resistance due to reduced contact area between the conducting particles. Additionally, the type of solvent used in composite preparation

### 3.1 Synthesis of Polyaniline and Polypyrrole

The method was similar to that described by Mattoso et al. [23] with a few changes. In a reactor of 1.5 L kept in the isotherm mode was added 900 mL of  $1.0 \text{ mol L}^{-1}$  of HCl and  $0.10 \text{ mol}$  of aniline and stirred at  $1 \text{ }^\circ\text{C}$  for 30 minutes. After that,  $0.025 \text{ mol}$  of ammonium persulfate (APS) previously solubilized in 100 milliliters of  $1.0 \text{ mol L}^{-1}$  HCl was mixed with the solution and kept the reaction for 2 hours. The solid was filtered and washed several times with  $0.25 \text{ mol L}^{-1}$  HCl. The solid was dried in a desiccator for one day and put into an oven at  $60 \text{ }^\circ\text{C}$  for 4 hours. The sample was referred to as PANi.

The polypyrrole synthesis was performed in similar conditions, although, no dopant was used. The sample was referred to as PPy.

### 3.2 Preparation of the composite samples

also influenced electrical conductivity, emphasizing the importance of considering solvent effects on the relationship between roughness and electrical resistance of materials [46,47]. However, it must be taken into account that the observed roughness pertains to the fracture regions of the samples, not to the regions where the measurement probes came into contact with the material for electrical conductivity measurements. This prevents us from making correlations between electrical conductivity measurements and contact angle data, morphology, and other parameters.

In another work, ABS was blended with PANi which was doped with different substances, camphor sulfonic acid (CSA) and dodecylbenzene sulfonic acid (DBSA). Due to the nature of these dopants, the miscibility was significantly enhanced, resulting in high electrical conductivity values DBSA demonstrated a ten-fold increase in electrical conductivity compared to CSA. It was noted that an increase in PANi content resulted in reduced flexibility, which ultimately impacted the bulk of the blend and impaired electrical conductivity [3].

## 3. Material and Methods

For the preparation of the test specimens, approximately ten grams of ABS were dissolved in 200 mL of acetone and heated to  $45 \text{ }^\circ\text{C}$ . Then, the specific amounts of 0.625, 1.25, 1.875, and 2.5 % (over the ABS mass) of conducting polymer (PANi or PPy) were added in a high torque mechanical stirrer at 1200 rpm for 2 hours at  $25 \text{ }^\circ\text{C}$ . After this step, the beakers with the mixtures were put in an isothermal bath at  $80 \text{ }^\circ\text{C}$  to evaporate the acetone under stirring until totally drying. Then, they were ground and placed in a mold with dimensions described according to ASTM D 638-M. The set was put in a thermal press under 5 tons at a temperature of  $150 \text{ }^\circ\text{C}$  for 2 minutes.

The samples were identified as pure ABS, ABS-PANi-X, and ABS-PANi-Y, where the letters X and Y are the numbers representing the percentage of mass of PANi and PPy over the total amount of ABS copolymer.

### 3.3 Scanning electron microscopy (SEM)

The samples were placed on support with carbon tape and then coated with metallic gold on an SCD050 (Leica) sputtering device. Next, the samples were analyzed by scanning electron microscopy EVO MA 10 (Carl Zeiss). Micrographs were obtained from the identical specimens tested in mechanical analysis. Micrographs were obtained of the sample surfaces and along the cross-section by fracturing under liquid nitrogen.

### 3.4 Mechanical analysis

In this assay, four specimens of each sample were tested. The stress-strain at break was determined with a universal machine Instron model 5982, cell charge of 5.0 kN. The 4-point method was used with the automatic speed of 2.0 mm min<sup>-1</sup>. The arrow in the center span was measured with an Instron LVDT, with a 5 mm course. The test specimens used in the mechanical strength analysis were according to ASTM D 638 M.

### 3.5 Thermogravimetric analysis (TGA)

The TGA measurements were performed in a SHIMADZU Model DTG-60H using a temperature range from 20 to 600 °C, in an inert atmosphere of N<sub>2(g)</sub> at 20 mL min<sup>-1</sup> with a heating rate of 10 °C min<sup>-1</sup>.

### 3.6 Contact angle

Contact angle measurements were performed using an equipment Theta Lite Optical Tensiometer, model TL100, with 60 frames per second CCD, and a syringe-type Hamilton, with 100 microliters of capacity with a volume drop of 5 microliters. The surface energies of the pure ABS and the composites were analyzed by contact angle (CA). Previously, the surfaces of the blends were cleaned with isopropyl alcohol and placed to dry in an oven with air ventilation at 60 °C for 6 hours. After this, the samples were placed in a desiccator under vacuum for 30 min. The contact angle measurements were performed as follows: the desired liquids were dripped onto the surface of the samples, and the equipment software calculated the contact angle formed between the liquid drop and the solid surface. The solvents used to measure the contact angles were deionized water, ethylene glycol (EG), N, N-dimethylformamide (DMF), and toluene. Calculations of the solid surface tension ( $\gamma_s$ ) and the dispersive ( $\gamma_s^d$ ) and polar ( $\gamma_s^p$ ) components were done by using the Owens-Wendt equation [24].

### 3.7 Electric resistance measurements

The electrical measurements of the pure ABS and blends follow the recommendations of Giroto and Santos [25]. The electrical assays were carried out at the Physics Institute at USP in São Carlos with an electrometer Keithley model 2636 B. Assay mode was a 4-wire type with a sketch where the electrodes always put the same pressure over the surface of samples. A distance of 5 mm was used between every two electrodes. The samples were cut in a circulus of 25 mm in diameter and 200 micrometers in thickness.

## 4. Conclusions

The analysis conducted in this study highlights the substantial impact of incorporating conductive polymers,

such as HCl-doped PANi and PPy, into ABS copolymer matrices. Fracture surface examinations revealed significant alterations in surface morphology attributed to the dispersion of these polymers, particularly evident in SEM images where PPy generated more aggregates compared to PANi, leading to rougher surfaces in ABS-PPy composites. Furthermore, the choice of solvent played a crucial role, with acetone acting as a nonsolvent for PPy. Mechanical tests indicated distinct trends in tensile and elasticity properties of ABS with varying levels of PANi and PPy, emphasizing the profound influence of these polymers on material behavior. Notably, even small additions of PANi or PPy resulted in considerable enhancements in electrical conductivity, with the most substantial improvements observed at 2.5% concentrations. Interestingly, the study also revealed a complex relationship between surface roughness and electrical resistance, with increased roughness potentially elevating resistance due to reduced contact area between conducting particles, particularly relevant for conducting surfaces. Additionally, the findings underscored the importance of solvent selection in composite preparation, further influencing electrical conductivity. It was possible to observe that even in small quantities, the presence of PANi or PPy contributes to increasing Young's modulus value, showing that there is a positive interaction between matrix and conductive polymers in a synergistic way. Even with a small amount of conductive polymers, under the percolation threshold, the electrical resistance decreases eleven-fold, which is a significant result for the application of these composites in electronic devices. Overall, these results provide valuable insights into optimizing the mechanical and electrical properties of ABS copolymers through the strategic incorporation of conductive polymers, paving the way for enhanced performance and broader application potential in electronic devices.

## Acknowledgments

The authors are grateful to the Minas Gerais State Research Funding Agency (FAPEMIG – processes CEX-APQ-01651-17, RED-00224-23), the Minas Chemical Network (RQ-MG), the Brazilian National Council for Scientific and Technological Development (CNPq, process 421974/2018-4), and the Coordination for the Improvement of Higher Education Personnel (CAPES) for financial support.

## Author Contributions

Bianca Taína Ferreira – Investigation, Methodology. Thamires Mariano – Data Curation, Formal Analysis. Gabriel Badagnani de Carvalho – Software, Visualization, Project Administration. Daniel Pasquini – Funding acquisition; Resources. Rondinele Alberto dos Reis Ferreira – Formal Analysis; Methodology; Software. Leila Aparecida de Castro Motta – Writing – Original Draft, Writing – Review & Editing. Luís Carlos de Moraes – Conceptualization; Funding acquisition; Investigation; Methodology; Project administration; Resources; Supervision; Visualization; Writing – review & editing.

## References and Notes

- [1] Ibrahim, B. A.; Kadum, K. M. *Mod. Appl. Sci.* **2010**, *4*, 161. [\[Crossref\]](#)
- [2] Malmonge, L. F.; Langiano, S. do C.; Cordeiro, J. M. M.;

- Mattoso, L. H. C.; Malmonge, J. A. *Mater. Res.* **2010**, *13*, 470. [\[Crossref\]](#)
- [3] Cristovan, F. H.; Lemos, S. G.; Pereira, E. C. *J. Appl. Polym. Sci.* **2009**, 831. [\[Crossref\]](#)
- [4] Ahmed, S. M. *Eur. Polym. J.* **2022**, *38*, 1158. [\[Crossref\]](#)
- [5] Giaconi, G. F.; Castellani, L.; Maestrini, C.; Riccò, T. *Polymer*, **1998**, *39*, 6324. [\[Crossref\]](#)
- [6] Zhang, H.; Ding, F.; Liu, T.; Liu, L.; Li, Y. *J. Appl. Polym. Sci.* **2021**, 139. [\[Crossref\]](#)
- [7] McNally, T.; Pötschke, P.; Halley, P.; Murphy, M.; Martin, D.; Bell, S. E. J.; Brennan, G. P.; Bein, D.; Lemoine, P.; Quinn. *Polymer*. **2005**, *46*, 8232. [\[Crossref\]](#)
- [8] Sandler, J. K. W.; Kirk, J. E.; Kinloch, I.A.; Shaffer M. S. P.; Windle, A. H. *Polymer*. **2003**, *44*, 5899. [\[Crossref\]](#)
- [9] Chen, Z.; Li, R.; Guo, Q. *Appl. Mech. Mater.* **2021**, 217-219, 1169. [\[Crossref\]](#)
- [10] Patil, R. C.; Kuratani, K.; Nakayama, M.; Ogura, K. *J. Polym. Sci.* **1999**, *37*, 2665. [\[Crossref\]](#)
- [11] Pud, A.; Ogurtsov, N.; Korzhenko, A.; Shapoval, G. *Prog. Polym. Sci.* **2003**, *28*, 1753. [\[Crossref\]](#)
- [12] Armes, S. P. *Synth. Met.* **1987**, *20*, 371. [\[Crossref\]](#)
- [13] Oh, E. J.; Jang, K.S.; Macdiarmid, A.G. *Synth. Met.* **2002**, *125*, 272. [\[Crossref\]](#)
- [14] Sinha, S.; Bhadra, S.; Khastgir, D. *J. Appl. Polym. Sci.* **2009**, *112*, 3140. [\[Crossref\]](#)
- [15] Blinova, N. V.; Stejskal, J.; Trchová, M.; Prokeš, J. *Polym Int.* **2008**, *57*, 69. [\[Crossref\]](#)
- [16] Skotheim, T.A.; Reynolds, J.R.; Handbook of Conducting Polymers, 3rd ed. CRC Press, Boca Raton, 1988. [\[Crossref\]](#)
- [17] Attia, N. F. *Polym. Adv. Technol.* **2016**, *27*, 1097. [\[Crossref\]](#)
- [18] Rubinger, C. P. L.; Leyva, M. E. *Polym. Bull.* **2018**, *76*, 626. [\[Crossref\]](#)
- [19] Huitrón-Gamboa J.A.; Encinas, J. C.; Castillo-Ortega, M.M. Castillo-Castro, T.; Santacruz-Ortega, H.; Rodríguez-Félix, D. E.; Manero, O. *Polym. Bull.* **2019**, *76*, 1965. [\[Crossref\]](#)
- [20] Irfan, M. S.; Gill, Y. Q.; Malik, S.; Neem, M. T.; Saeed, F.; Hashmi, M. *Smart. Mater. Struct.* **2019**, *28*. [\[Crossref\]](#)
- [21] Shakir, M. F.; Tariq, A.; Rehan, Z.A.; Nawab, Y.; Rashid, I. A.; Afsal, A.; Hamid, U.; Raza, F.; Aubair, K.; Rizwan, M. S.; Riaz, S.; Sultan, A.; Mauttaqi, M. *SN. Appl. Sci.* **2020**, *2*. [\[Crossref\]](#)
- [22] Foulger, S.H. *J. Polym. Sci., Part B: Polym. Phys.* **1999**, *37*, 1910. [\[Crossref\]](#)
- [23] Mattoso, L. H. C.; Macdiarmid, A. G.; Epstein, A. J. *Synth Met.* **1994**, *68*, 11. [\[Crossref\]](#)
- [24] Owens, D. K.; Wendt, R.C. *J. Appl. Polym. Sci.* **1969**, *13*, 1747. [\[Crossref\]](#)
- [25] Giroto, E.M.; Santos, I.A. *Quim. Nova*, **2002**, *25*, 647. [\[Crossref\]](#)
- [26] Bernal, C.R.; Frontini, P. M.; Sforza, M.; Bibbó, M.A. *J. Appl. Polym. Sci.* **1995**, *58*, 10. [\[Crossref\]](#)
- [27] Simunec, D. P.; Sola, A. *Adv. Eng. Mater.* **2022**, *24*. [\[Crossref\]](#)
- [28] Shackletfe, L.W.; Han, C.C. *Mat. Res. Soc. Symp. Proc.* **1994**, *328*, 166. [\[Crossref\]](#)
- [29] Li, W.; Wan, M. *Synt. Met.* **1998**, 126. [\[Crossref\]](#)
- [30] Peng, P.; Shi, B.; Jia, L.; Li, B. *J. Macromol. Sci., Part B: Phys.* **2010**, *49*, 869. [\[Crossref\]](#)
- [31] Wypych, G. Handbook of solvents. ChemTec, New York, 2001.
- [32] Merlini, C.; Barra, G. M. D. O.; Araujo, T. M., Pegoretti, A. *Synth. Met.* **2014**, 192. [\[Crossref\]](#)
- [33] Wen, Q.; Pan, X.; Hu, Q.; Zhao, S.; Hou, Z.; Yu, Q. *Synth. Met.* **2013**, *164*, 31. [\[Crossref\]](#)
- [34] Pospiech, D.; Gottwald, A.; Jehnichen, D.; Friedel, P.; John, A.; Harnisch, C.; Voigst, D.; Khimich, G.; Bilibin, A. *Y. Colloid. Polym. Sci.* **2002**, *280*, 1037. [\[Crossref\]](#)
- [35] Mori, S.; Barth, H. G. Size Exclusion Chromatography. 1st ed. New York: Springer 1999. [\[Crossref\]](#)
- [36] Greco, R.; Dong, L. *Macromol. Symp.* **1994**, *78*, 153. [\[Crossref\]](#)
- [37] Debnath, N.; Panwar, V.; Bag, S.; Saha, M.; Pal, K. *J. Appl. Polym. Sci.* **2015**, *132*, 7. [\[Crossref\]](#)
- [38] Kumar, A.; Kumar, A.; Mudila, H.; Awasthi, K.; Kumar, V. *J. Phys.: Conf. Ser.* **2020**, 1531. [\[Crossref\]](#)
- [39] Yussuf, A.; Al-Saleh, M.; Al-Enezi, S.; Abraham, G. *Int. J. Polym. Sci.* **2018**, *8*. [\[Crossref\]](#)
- [40] Belgacem, M.N.; Gandini, A. *Compos. Interfaces.* **2005**, *12*, 75. [\[Crossref\]](#)
- [41] Magallón Cacho, L.; Pérez Bueno, J. J.; Meas Vong, Y.; Stremdoerfer, G.; Espinoza Beltrán, F. J.; Martínez Vega, J. *J. Coat. Technol. Res.* **2015**, *12*, 323. [\[Crossref\]](#)
- [42] Olivera, S.; Muralidhara, H. B.; Venkatesh, K.; Gopalakrishna, K.; Vivek, C. S. *J. Mater. Sci.* **2016**, *51*, 3674. [\[Crossref\]](#)
- [43] Wypych, G.; Pionteck, J. Handbook of antistatics, 2nd ed. Toronto: ChemTec, 2016.
- [44] Ahmed, S. M. *Eur. Polym. J.* **2002**, *38*, 1158. [\[Crossref\]](#)
- [45] Vicentini, D. S.; Barra, G. M. O.; Bertolino, J. R.; Pires, A. T. N. *Eur. Polym. J.* **2007**, *43*, 4572. [\[Crossref\]](#)
- [46] Namsheer, K.; Chandra, S. R. *RSC Adv.* **2021**, *11*, 5697. [\[Crossref\]](#)
- [47] Ding, H.; Hussein, A. M.; Ahmad, I.; Latef, R.; Abbas, J. K.; Ali, A. T. A.; Saeed, S. M.; Adbulwahid, A. S.; Ramandan, M. F.; Rasol, H. A.; Elawady, A. *Alex. Eng. J.* **2024**, *88*, 267. [\[Crossref\]](#)

## How to cite this article

Ferreira, B. T.; Mariano, T.; de Carvalho, G. B.; Pasquini, D.; Ferreira, R. A. R.; Motta, L. A. C.; de Moraes, L. C. *Orbital: Electron. J. Chem.* **2024**, *16*, 143. <http://dx.doi.org/10.17807/orbital.v16i3.19917>